J|A|C|S
ARTICLES

Published on Web 12/07/2010

Mechanistic Studies of Peptide Self-Assembly: Transient α-Helices to Stable β-Sheets

Gai Liu,[†] Anabathula Prabhakar,[†] Darryl Aucoin,[†] Miranda Simon,[†] Samuel Sparks,[†] Kevin J. Robbins,[†] Andrew Sheen,[†] Sarah A. Petty,[‡] and Noel D. Lazo*[,†]

Carlson School of Chemistry and Biochemistry, Clark University, 950 Main Street, Worcester, Massachusetts 01610, and Department of Chemistry, College of the Holy Cross, 1 College Street, Worcester, Massachusetts 01610

Received August 4, 2010; E-mail: nlazo@clarku.edu

Abstract: The pathologic self-assembly of proteins is associated with typically late-onset disorders such as Alzheimer's disease, Parkinson's disease, and type 2 diabetes. Important mechanistic details of the self-assembly are unknown, but there is increasing evidence supporting the role of transient α-helices in the early events. Islet amyloid polypeptide (IAPP) is a 37-residue polypeptide that self-assembles into aggregates that are toxic to the insulin-producing β cells. To elucidate early events in the self-assembly of IAPP, we used limited proteolysis to identify an exposed and flexible region in IAPP monomer. This region includes position 20 where a serine-to-glycine substitution (S20G) is associated with enhanced formation of amyloid fibrils and early onset type 2 diabetes. To perform detailed biophysical studies of the exposed and flexible region, we synthesized three peptides including IAPP(11-25)WT (wild type), IAPP(11-25)S20G, and IAPP(11-25)S20P. Solution-state NMR shows that all three peptides transiently populate the α-helical conformational space, but the S20P peptide, which does not self-assemble, transiently samples a broken helix. Under similar sample conditions, the WT and S20G peptides populate the α-helical intermediate state and β-sheet end state, respectively, of fibril formation. Our results suggest a mechanism for self-assembly that includes the stabilization of transient α-helices through the formation of NMR-invisible helical intermediates followed by an α-helix to β-sheet conformational rearrangement. Furthermore, our results suggest that reducing intermolecular helix−helix contacts as in the S20P peptide is an attractive strategy for the design of blockers of peptide self-assembly.

Introduction

The self-assembly of the amyloid β-protein (Aβ), α-synuclein (α-syn), and islet amyloid polypeptide (IAPP) is associated with Alzheimer's disease (AD), Parkinson's disease (PD), and type 2 diabetes (T2D), respectively. In each case, the precursor protein self-assembles into insoluble and stable amyloid fibrils through a hierarchical process that generates toxic species. Over the past few decades, productive efforts by several research groups have demonstrated that, notwithstanding the differences in primary structure, the self-assembly of Aβ, α-syn, and IAPP share common features. The monomeric states of the three proteins are more compact than an ideal random coil conformation, suggesting that parts of the proteins may be unavailable for the formation of initial intermolecular contacts.[1−3] The self-assembly is cooperative in the sense that fibril formation is accelerated once the critical oligomeric nucleus is formed.[4] When self-assembly in hydro is monitored by circular dichroism (CD), the three proteins display random coil → α-helix → β-sheet conformational transitions.[5−7] In the presence of model membranes, they readily form helical structures which then convert to β-sheets.[8] The fibrils adopt the cross-β-sheet structure, first proposed by Pauling and Corey for silk,[9] in which the β-strands and β-sheets are oriented perpendicular and parallel, respectively, to the fibril axis.

Here, we focus on the self-assembly of IAPP, a 37-residue polypeptide co-secreted with insulin by pancreatic β cells. A serine-to-glycine substitution in position 20 (S20G) of the polypeptide leads to early-onset T2D.[10] Post mortem evaluations of T2D patients showed that 90% had extracellular amyloid plaques in their pancreas that are composed mostly of IAPP fibrils.[11] IAPP fibrils are toxic to cells,[12,13] so the fibrils found in the pancreas may be responsible for β-cell death and

[†] Clark University.
[‡] College of the Holy Cross.

(1) Dupuis, N. F.; Wu, C.; Shea, J. E.; Bowers, M. T. *J. Am. Chem. Soc.* **2009**, *131*, 18283–18292.
(2) Lazo, N. D.; Grant, M. A.; Condron, M. C.; Rigby, A. C.; Teplow, D. B. *Protein Sci.* **2005**, *14*, 1581–1596.
(3) Bernado, P.; Bertoncini, C. W.; Griesinger, C.; Zweckstetter, M.; Blackledge, M. *J. Am. Chem. Soc.* **2005**, *127*, 17968–17969.
(4) Wetzel, R. *Acc. Chem. Res.* **2006**, *39*, 671–679.
(5) Kirkitadze, M. D.; Condron, M. M.; Teplow, D. B. *J. Mol. Biol.* **2001**, *312*, 1103–1119.
(6) Knight, J. D.; Hebda, J. A.; Miranker, A. D. *Biochemistry* **2006**, *45*, 9496–9508.
(7) Zhu, M.; Li, J.; Fink, A. L. *J. Biol. Chem.* **2003**, *278*, 40186–40197.
(8) Hebda, J. A.; Miranker, A. D. *Annu. Rev. Biophys.* **2009**, *38*, 125–152.
(9) Pauling, L.; Corey, R. *Proc. Natl. Acad. Sci. U.S.A.* **1951**, *37*, 729–739.
(10) Sakagashira, S.; Sanke, T.; Hanabusa, T.; Shimomura, H.; Ohagi, S.; Kumagaye, K. Y.; Nakajima, K.; Nanjo, K. *Diabetes* **1996**, *45*, 1279–1281.
(11) Westermark, P. *Upsala J. Med. Sci.* **1972**, *77*, 91–94.
(12) Lorenzo, A.; Razzaboni, B.; Weir, G. C.; Yankner, B. A. *Nature* **1994**, *368*, 756–760.

dysfunction in late stages of the disease.[14] More recent in vitro toxicity studies suggest, however, that soluble oligomers, as opposed to fibrils, are primarily responsible for the IAPP-induced cytotoxicity.[8,15−17] If true, then a therapeutic strategy that is more attractive than one that targets fibrils suggests itself: design small molecules that inhibit the formation of oligomeric assemblies. This requires knowledge of the monomeric state of IAPP and the ensuing early events of self-assembly.

Previous NMR studies of IAPP monomer in hydro suggest the presence of transient α-helices.[18−21] The role of transient α-helices in self-assembly is poorly understood. Here, we begin by identifying a region in IAPP monomer from which the initial intermolecular contacts necessary for oligomer formation may arise. To perform detailed biophysical studies of this region, we synthesized three peptides including IAPP(11-25)WT (wild type), IAPP(11-25)S20G, and IAPP(11-25)S20P. The monomeric states of the three peptides transiently populate the α-helical conformational space. However, their abilities to self-assemble are dramatically different. The implications of these results for peptide self-assembly and its abolishment are discussed.

Methods

Peptide Synthesis. The peptides used here were synthesized by standard solid-phase peptide synthesis using 9-fluorenylmethoxycarbonyl (FMOC) chemistry. All FMOC-protected amino acids and resins were purchased from EMD Chemicals Inc. (Gibbstown, NJ). To minimize the aggregation of full-length IAPP during synthesis, pseudoproline dipeptide derivatives were used at three locations as described previously.[22] All IAPP(11-25) peptides were purified in house by reversed-phase HPLC and characterized by mass spectrometry at the University of Massachusetts Medical School. After synthesis, full-length IAPP was sent to Biomer Technology (Pleasanton, CA) for disulfide bond formation and purification.

Sample Preparation. Dry purified peptide was dissolved in ice-cold 10 mM phosphate buffer of variable pH (vide infra). To remove aggregates, a two-step procedure that included centrifugation at 16000 × *g* for 30 s immediately followed by a careful transfer of the clear supernatant to clean tubes was done three times. The final supernatant was used for limited proteolysis, circular dichroism (CD), or NMR. To ensure that this method yields aggregate-free IAPP(11-25) solutions, representative samples were analyzed by dot blot assay using the antioligomer antibody A11 (Invitrogen) as described elsewhere.[23] Peptide concentrations were determined by UV absorbance at 214 nm using calculated extinction coefficients.[24]

Limited Proteolysis. Limited proteolysis experiments were done as described elsewhere.[2,25] Enzymatic digestions of IAPP at pH 5.5 or 7.4 were done at 25 °C using thermolysin (TH) (Sigma-Aldrich) or human neutrophil elastase (HNE) (Calbiochem) at a substrate to enzyme ratio of 100:1. Eighteen microliters of each digestion was removed periodically to which 8 μL of 1% trifluoroacetic acid in water (v/v) was added to quench the reaction. All samples were zip tipped using Omix C18 pipet tips (Varian, Inc.) for peptide desalting and then stored at −20 °C.

Mass Spectrometry. All mass spectra were obtained at the Mass Spectrometry Facility of the University of Massachusetts Medical School using a Finnigan LTQ linear quadrupole IT MS system (Thermo Fisher Scientific, MA). This was operated in data-dependent triple play mode with one full survey scan (*m*/*z* 200−2000), followed by a zoom scan and a product ion scan of the zoom-scanned ion.

Circular Dichroism. All far-UV CD spectra were acquired at 4 °C using a JASCO J-815 spectropolarimeter. A quartz cuvette with a path length of 1 mm was used in all experiments. Spectra are the average of four repeats, with each repeat recorded over a wavelength range of 260 to 200 or 195 nm, at intervals of 1 nm and an averaging time of 4 s. All CD samples were kept at 4 °C in between acquisition of spectra.

Thioflavin T Fluorescence. A solution of thioflavin T in 10 mM phosphate buffer (pH 4.3) at a concentration of 14 μM was prepared. To prepare a sample for fluorescence, an aliquot of the peptide solution was added to the ThT solution such that the final peptide concentration was 7 μM. Fluorescence was measured using a Perkin-Elmer LS50B luminescence spectrometer. Spectra at 0, 3, 6, 10, and 20 days were obtained for the three peptides. Three fluorescence samples per peptide were prepared at each time point, and the average of the three spectra is reported here. All emission spectra were measured from 450 to 600 nm, following excitation at 440 nm. The excitation and emission slit widths were set at 10 nm.

Congo Red Binding. The ability of the IAPP(11-25) peptides incubated for 20 days at 4 °C to bind Congo red was tested using UV absorbance as described elsewhere.[26] Briefly, an aliquot of the sample was added to 240 μL of 25 μM Congo red in 10 mM phosphate buffer (pH 4.3) such that the final peptide concentration was 6 μM. After 30 min of incubation at room temperature, a UV absorbance spectrum was acquired using a Varian 50Bio UV−vis spectrophotometer.

Transmission Electron Microscopy. Electron microscopy was performed at the Core Electron Microscopy Facility of the University of Massachusetts Medical School. Aliquots were taken periodically from the CD and NMR samples. Each was placed on a carbon-coated copper grid and stained with 1% uranyl acetate for 2 min.

Fourier Transform Infrared Spectroscopy. FTIR spectra were collected on a Bruker Tensor 37 FTIR spectrometer operating at a resolution of 2 cm^{-1}. The exposed amide protons of the peptides were first exchanged for deuterium by dissolving in D_2O and lyophilizing twice. The sample was then dissolved in deuterated sodium phosphate buffer (pH 7.5) to a final concentration of approximately 20 mg/mL and was placed in an IR cell fitted with two CaF_2 windows separated by a 100 μm Teflon spacer. Then, 512 IR spectra were collected and averaged at 25 and 45 °C; temperature was regulated by means of a water jacket connected to an external water bath and was allowed to equilibrate for 10 min before measurements were taken. Additionally a spectrum was collected after prolonged incubation at 45 °C to ensure equilibrium had been reached and no further changes were occurring. Analysis of the data focused on the amide I mode, which is due primarily to

(13) Engel, M. F.; Khemtemourian, L.; Kleijer, C. C.; Meeldijk, H. J.; Jacobs, J.; Verkleij, A. J.; de Kruijff, B.; Killian, J. A.; Hoppener, J. W. *Proc. Natl. Acad. Sci. U.S.A.* **2008**, *105*, 6033–6038.
(14) Kahn, S. E.; Andrikopoulos, S.; Verchere, C. B. *Diabetes* **1999**, *48*, 241–253.
(15) Jayasinghe, S. A.; Langen, R. *Biochim. Biophys. Acta* **2007**, *1768*, 2002–2009.
(16) Haataja, L.; Gurlo, T.; Huang, C. J.; Butler, P. C. *Endocr. Rev.* **2008**, *29*, 303–316.
(17) Engel, M. F. *Chem. Phys. Lipids* **2009**, *160*, 1–10.
(18) Williamson, J. A.; Miranker, A. D. *Protein Sci.* **2007**, *16*, 110–117.
(19) Yonemoto, I. T.; Kroon, G. J.; Dyson, H. J.; Balch, W. E.; Kelly, J. W. *Biochemistry* **2008**, *47*, 9900–9910.
(20) Williamson, J. A.; Loria, J. P.; Miranker, A. D. *J. Mol. Biol.* **2009**, *393*, 383–396.
(21) Cort, J. R.; Liu, Z.; Lee, G. M.; Huggins, K. N.; Janes, S.; Prickett, K.; Andersen, N. H. *Protein Eng., Des. Sel.* **2009**, *22*, 497–513.
(22) Abedini, A.; Raleigh, D. P. *Biochemistry* **2005**, *44*, 16284–16291.
(23) Necula, M.; Kayed, R.; Milton, S.; Glabe, C. G. *J. Biol. Chem.* **2007**, *282*, 10311–10324.
(24) Kuipers, B. J.; Gruppen, H. *J. Agric. Food Chem.* **2007**, *55*, 5445–5451.
(25) Grant, M. A.; Lazo, N. D.; Lomakin, A.; Condron, M. M.; Arai, H.; Yamin, G.; Rigby, A. C.; Teplow, D. B. *Proc. Natl. Acad. Sci. U.S.A.* **2007**, *104*, 16522–16527.
(26) Klunk, W. E.; Pettegrew, J. W.; Abraham, D. J. *J. Histochem. Cytochem.* **1989**, *37*, 1273–1281.

the carbonyl stretching vibration of the amino acids and is known to be a useful indicator of peptide secondary and tertiary structures. The spectra were first normalized to the height of the peak at 1674 cm^{-1}, which is indicative of residual trifluoroacetic acid, and were then fit to the sum of three pseudo-Voigt bands using a nonlinear least squares (Levenberg−Marquardt) fitting routine (in MicroCal Origin). This fit approximates the convolution of Gaussian and Lorentzian functions to the weighted addition of the two functions using a common center frequency and width and has been used previously for simplification purposes.[27]

NMR Spectroscopy. All NMR experiments were performed at 4 °C on a Varian INOVA spectrometer operating at 600 MHz (proton frequency) and equipped with a 5 mm, pulsed-field gradient triple-resonance probe. Both one-dimensional (1D) and two-dimensional (2D) ^{1}H NMR spectra were recorded, all of which were referenced with respect to the methyl peak of 2,2-dimethyl-2-silapentane-5-sulfonate (DSS). Two-dimensional total correlation spectroscopy (TOCSY) spectra were acquired with a mixing time of 80 ms using the MLEV-17 spin−lock sequence[28] to drive the coherence transfer. Two-dimensional rotating-frame Overhauser enhancement spectroscopy (ROESY)[29] spectra were obtained using mixing times of 300 and 400 ms. All 2D spectra were acquired in the phase-sensitive mode. To reduce the water peak in 2D spectra, WATERGATE suppression[30] was used. The ^{1}H resonance spin systems were assigned from analysis of TOCSY spectra. Sequential assignments were made by locating d_{NN} and $d_{\alpha N}$ connectivities in the ROESY spectra. After spectral acquisition, all NMR samples were stored at 4 °C.

To determine the extent of aggregation as a function of time, we collected a series of TOCSY spectra. The relative volume of each NH → H^{α} cross peak was measured, using the volume of the DSS peak, which does not change with incubation time, as the reference volume. The ratio defined by (cross-peak volume at day *X*)/(cross-peak volume at day 0) was calculated. The ratios were then averaged over all residues. The average, taken to indicate monomer abundance (vide infra), was then plotted against incubation time.

Results and Discussion

Identification of an Exposed and Flexible Region in Full-Length IAPP Monomer. Amyloidogenic oligomers are stabilized by noncovalent interactions between two or more monomers. An attractive approach in inhibitor design, therefore, is to disrupt the noncovalent interactions in a manner that oligomer formation is abolished. This requires identification of recognition sites in the monomer from which such interactions may arise. These sites must be exposed and flexible to participate in self-assembly. An experimental technique that can determine the exposed and flexible parts of proteins that have a propensity to aggregate is limited proteolysis monitored by mass spectrometry (LP/MS).[2,25,31,32] The premise of limited proteolysis is simple: peptide bond cleavage requires a sequence that is recognized by the protease and the accessibility of that sequence for cleavage. The requirement for the latter is exposure and a flexible or unstructured conformation that can easily bind and adapt to the active site of the enzyme.[33] Two important advantages of LP/MS are that the concentration of protein required is low and that the structural information can be obtained within minutes of sample preparation.

Table 1. Initial Cleavage Sites in Human IAPP Determined from LP/MS Experiments Using Thermolysin (TH) and Human Neutrophil Elastase (HNE) at a Substrate to Enzyme Ratio of 100:1 in 10 mM Sodium Phosphate Buffer (pH 7.4) at 25 °C

cleavage site	enzyme	fragment	observed mass, Da	calculated mass, Da	Δ(obsd mass − calcd mass), Da
Arg11-Leu12	TH	1−11	1193.7	1194.4	−0.7
		12−37	2727.2	2727.0	0.2
Asn14-Phe15	TH	1−14	1491.8	1492.7	−0.9
		15−37	2428.2	2428.7	−0.5
Phe15-Leu16	TH	1−15	1639.7	1639.9	−0.2
		16−37	2281.1	2281.5	−0.4
Asn22-Phe23	TH	1−22	2391.5	2391.7	−0.2
		23−37	1529.7	1529.7	0
Val17-His18	HNE	1−17	1851.6	1852.2	−0.6
		18−37	2086.1	2086.3	−0.2

Results of LP/MS of IAPP at 25 °C and pH 7.4 using HNE, an enzyme specific for Val−X peptide bonds, and TH, a nonspecific enzyme, are shown in Table 1. Identical results were obtained when the digestions were conducted at pH 5.5, at the lower limit of enzyme activity and close to the pH used in the biophysical studies (Table S1 in the Supporting Information). Figure 1 shows the peptide bonds in IAPP monomer susceptible to proteolysis. Both N- and C-terminal regions of IAPP are protected against proteolytic attack. The central part of IAPP, however, contains five initial cleavage sites, including the Phe23−Gly24 peptide bond found in the 22−27 region identified as the most amyloidogenic in IAPP.[34] This result suggests that the central region of IAPP is exposed and flexible and thus may contain the recognition sites required for the initial events in self-assembly. This correlates nicely with peptide mapping studies showing maximum binding of full-length IAPP to IAPP(11-20),[35] acceleration of fibril formation by full-length IAPP in the presence of IAPP(15-20),[36] inhibition of fibril formation by proline substitutions in the 14−20 region,[37] and binding and computational docking experiments which identified Ala8−His18 as the region responsible for the formation of IAPP dimers.[38]

The N-terminal region of IAPP is protected against proteolysis by TH, presumably because of the presence of the disulfide bond between Cys2 and Cys7 which may prevent its interaction with the active site of the enzyme. To explain the protection of the C-terminal region, we considered two possibilities: First, it is plausible that parts of the C-terminus are involved in intermolecular interactions that may be true if IAPP oligomers are being proteolyzed. Previous studies by others have identified the segment $N_{22}FGAIL_{27}$ as the amyloid core sequence of IAPP.[39] Indeed, when Gly24 and Ile26 in this region are N-methylated (i.e., the backbone NH is modified to $N-CH_3$ to produce a double N-methylated full-length IAPP [$(N-CH_3)$G24, $(N-CH_3)$I26-IAPP]), the IAPP analogue becomes highly soluble, nonamy-

(27) Chirgadze, Y. N.; Shestopalov, B. V.; Venyaminov, S. Y. *Biopolymers* **1973**, *12*, 1337–1351.
(28) Bax, A.; Davis, D. G. *J. Magn. Reson.* **1985**, *65*, 355–360.
(29) Hwang, T. L.; Shaka, A. J. *J. Am. Chem. Soc.* **1992**, *114*, 3157–3159.
(30) Piotto, M.; Saudek, V.; Sklenar, V. *J. Biomol. NMR* **1992**, *2*, 661–665.
(31) Kheterpal, I.; Williams, A.; Murphy, C.; Bledsoe, B.; Wetzel, R. *Biochemistry* **2001**, *40*, 11757–11767.
(32) Polverino de Laureto, P.; Taddei, N.; Frare, E.; Capanni, C.; Costantini, S.; Zurdo, J.; Chiti, F.; Dobson, C. M.; Fontana, A. *J. Mol. Biol.* **2003**, *334*, 129–141.
(33) Hubbard, S. J. *Biochim. Biophys. Acta* **1998**, *1382*, 191–206.
(34) Yan, L. M.; Tatarek-Nossol, M.; Velkova, A.; Kazantzis, A.; Kapurniotu, A. *Proc. Natl. Acad. Sci. U.S.A.* **2006**, *103*, 2046–2051.
(35) Mazor, Y.; Gilead, S.; Benhar, I.; Gazit, E. *J. Mol. Biol.* **2002**, *322*, 1013–1024.
(36) Scrocchi, L. A.; Ha, K.; Chen, Y.; Wu, L.; Wang, F.; Fraser, P. E. *J. Struct. Biol.* **2003**, *141*, 218–227.
(37) Abedini, A.; Raleigh, D. P. *J. Mol. Biol.* **2006**, *355*, 274–281.
(38) Wiltzius, J. J.; Sievers, S. A.; Sawaya, M. R.; Eisenberg, D. *Protein Sci.* **2009**, *18*, 1521–1530.
(39) Kapurniotu, A.; Schmauder, A.; Tenidis, K. *J. Mol. Biol.* **2002**, *315*, 339–350.

Figure 1. Exposed and flexible regions in IAPP monomer. LP/MS of IAPP monomer identified five initial cleavage sites. The unshaded arrow indicates the peptide bond cut by human neutrophil elastase (HNE), while the shaded arrows indicate peptide bonds cleaved by thermolysin (TH).

loidogenic, and nontoxic.[34] Taking together these published works and our LP/MS results showing peptide bond cleavages in the molecular recognition motif and in the amyloid core sequence (Figure 1), we conclude that IAPP monomers are being proteolyzed. Second, it is possible that parts of the C-terminus participate in intramolecular interactions. We noted that the C-terminus contains a Val-Gly-Ser-Asn sequence that is also found in a 10-residue region of Aβ that is resistant to proteolytic attack.[2] Experimental[2,25] and computational studies[40] of this region indicate the presence of a five-residue turn centered at Gly-Ser-Asn, similar to that found in models of Aβ fibrils.[41,42] We speculate that a similar turn or turnlike structure is present in the C-terminus of IAPP.

Biophysical Studies of Self-Assembly by Peptides Containing the Exposed and Flexible Region of IAPP. To allow for detailed biophysical studies of the region of IAPP that may be involved in the formation of the initial intermolecular contacts, a 15-residue peptide designated as IAPP(11-25)WT (wild type) (acetyl-RLANFLVHSSNNFGA-NH_2) was synthesized. This peptide contains all protease-accessible peptide bonds identified in Figure 1 and the 11−20 fragment previously identified by others as the key molecular recognition domain of IAPP.[35] Two other peptides were studied: IAPP(11-25)S20G (acetyl-RLANFLVHS*G*NNFGA-NH_2), which contains the S20G mutation, and IAPP(11-25)S20P (acetyl-RLANFLVHS*P*NNFGA-NH_2), which contains proline at position 20. All peptides were studied at pH 4.3, similar to the moderately acidic environment (pH ∼5.5) of IAPP in β-cell secretory granules.[43] Also, at pH 4.3, the lone histidine residue (His18) ($pK_a \sim 6.0$) is protonated, which should increase peptide solubility.[22] Freshly prepared solutions of these peptides were found to be oligomer-free by the dot blot assay using the antioligomer antibody A11 (Figure S1 in the Supporting Information).

Assembly Competence. Far-UV CD spectroscopy was used to test for the competence of the IAPP(11-25) peptides for self-assembly. Immediately after sample preparation, the three peptides displayed CD spectra typical of random coil peptides, i.e., a strong negative band near 200 nm and a very weak band above 210 nm (Figure 2). After 20 days of incubation at 4 °C, IAPP(11-25)WT and IAPP(11-25)S20G displayed CD spectra consistent with the dominant presence of ordered peptide assemblies. In contrast, IAPP(11-25)S20P remained disordered. This result is consistent with previous studies showing that when proline is placed in positions critical for β-sheet formation, amyloid formation is abolished.[44−46] TEM of the 20-day old CD samples showed that IAPP(11-25)S20G formed more

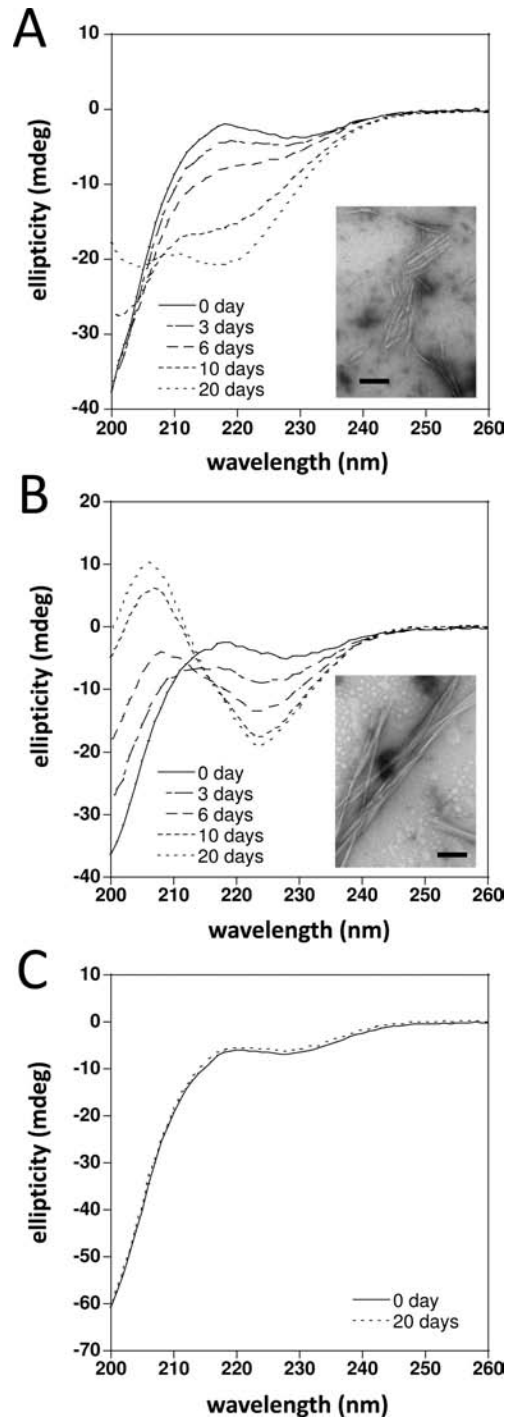

Figure 2. Competence of the IAPP(11-25) peptides for self-assembly. Far-UV CD spectra of (A) IAPP(11-25)WT, (B) IAPP(11-25)S20G, and (C) IAPP(11-25)S20P in 10 mM sodium phosphate buffer (pH 4.3, 4 °C). All peptides are predominantly unstructured initially. After 20 days of incubation at 4 °C, the S20G and WT peptides formed assemblies that are primarily β-sheet- and α-helix-rich, respectively. The S20P peptide remained unstructured. The peptide concentrations are 133, 132, and 287 μM for WT, S20G, and S20P, respectively, similar to those used in the NMR studies. Insets show TEM images of assemblies present in the 20-day-old CD samples. Scale bars are 100 nm.

assemblies than IAPP(11-25)WT and that most of them are fibrils with indeterminate lengths. Some fibrils bundled together to form thicker assemblies (Figure 2B). The assemblies formed by IAPP(11-25)WT, on the other hand, are mostly short with

(40) Murray, M. M.; Krone, M. G.; Bernstein, S. L.; Baumketner, A.; Condron, M. M.; Lazo, N. D.; Teplow, D. B.; Wyttenbach, T.; Shea, J. E.; Bowers, M. T. *J. Phys. Chem. B* **2009**, *113*, 6041–6046.
(41) Petkova, A. T.; Ishii, Y.; Balbach, J. J.; Antzutkin, O. N.; Leapman, R. D.; Delaglio, F.; Tycko, R. *Proc. Natl. Acad. Sci. U.S.A.* **2002**, *99*, 16742–16747.
(42) Luhrs, T.; Ritter, C.; Adrian, M.; Riek-Loher, D.; Bohrmann, B.; Dobeli, H.; Schubert, D.; Riek, R. *Proc. Natl. Acad. Sci. U.S.A.* **2005**, *102*, 17342–17347.
(43) Orci, L.; Halban, P.; Perrelet, A.; Amherdt, M.; Ravazzola, M.; Anderson, R. G. *J. Cell Biol.* **1994**, *126*, 1149–1156.

determinate lengths (~70−330 nm) (Figure 2A), typical of assembly intermediates.

Secondary Structure Content of Assemblies. We noted that the day-20 CD spectrum of IAPP(11-25)WT has two minima (Figure 2A) similar to reported spectra of α-helix-rich assemblies formed by Aβ,[5] IAPP,[6,47] and α-synuclein.[7] At a lower peptide concentration, spectra which show the rise in ellipticity near 200 nm, consistent with spectra of α-helix-rich assemblies,[5−7,47] were obtained (Figure S2 in the Supporting Information). The day-20 CD spectrum of IAPP(11-25)S20G, on the other hand, is similar to spectra of model β-sheets (Figure 2B). However, the minimum is red shifted by 8 nm to 224 nm, likely due to light scattering by the fibrils.[48] Because of this and the absence of a suitable reference database, current algorithms that have been used successfully to deconvolute CD spectra of unaggregated proteins may be unreliable for IAPP assemblies.

An alternative method is FTIR, which is more sensitive to β-sheet than CD. Figure 3A shows that there are clear differences between the FTIR spectra of assemblies from IAPP(11-25)WT and IAPP(11-25)S20G. Results of a three three-band pseudo-Voigt fit to the spectra are shown in Figure 3B,C. This fitting routine has been used previously to allow the simplification of a true Voigt fit[27,49,50] and for Gaussian broadening (due to an inhomogeneity in the interactions with the solvent) of the intrinsically Lorentzian infrared bands.[27] The quality of these fits is assessed in the MicroCal Origin fitting routine and is reported as an adjusted coefficient of determination (Adj R^2) which takes into account both the deviation of the data from the fit and the degrees of freedom included in the fit; thus, improving the visual appearance of the fit simply by adding additional parameters does not guarantee an improvement in the adjusted coefficient of determination. In the fit results shown in Figure 3, Adj R^2 values of 0.999 62 (Figure 3B) and 0.990 42 (Figure 3C) were obtained, indicating high correlations between the fit and the data (a perfect fit would yield Adj R^2 = 1). To ensure these results represented the best deconvolution, the fit was rerun several times from different starting parameters; once all parameters were allowed to vary freely, the fit converged to the same end point. In both cases the band at 1674 cm^{-1} indicates the presence of residual trifluoroacetic acid, as previously established.[51,52] The remaining two bands, at 1654 and 1622 cm^{-1} in the wild-type peptide and at 1661 and 1623 cm^{-1} in the S20G mutant, are indicative of different elements of secondary structure.

The peak at 1622−1623 cm^{-1} is assigned to β-sheet based on its shape and frequency: β-sheet peaks are typically very Lorentzian in nature[53,54] due to the highly ordered nature of the structure which limits the inhomogeneity of solvent interactions associated with Gaussian broadening; in Figure 3B,C, the band at 1622−1623 cm^{-1} is entirely Lorentzian (fixing the peak to a Gaussian shape decreases the value of Adj R^2 notably, and allowing it to vary freely yields the Lorentzian band shown). The frequency of this band is consistent with previously collected spectra of β-sheet proteins and peptides: A vibrational frequency of 1622−1623 cm^{-1} has been previously assigned to parallel β-strands in full length IAPP,[55] to β-sheets within the parallel β-helical protein UDP-*N*-acetylglucosamine acyltransferase,[56] to β-sheets in a 13-residue peptide (KLEG13)[56] whose CD spectrum is suggestive of β-helix formation and which has been seen by electron microscopy to form fibrils,[57] and to β-sheet structure in concanavalin A by Byler and Susi.[58] This peak is the minor band in the spectrum of IAPP(11-25)WT representing 18% of the total area assigned to peptide backbone vibrations but is the dominant band in the spectrum of IAPP(11-

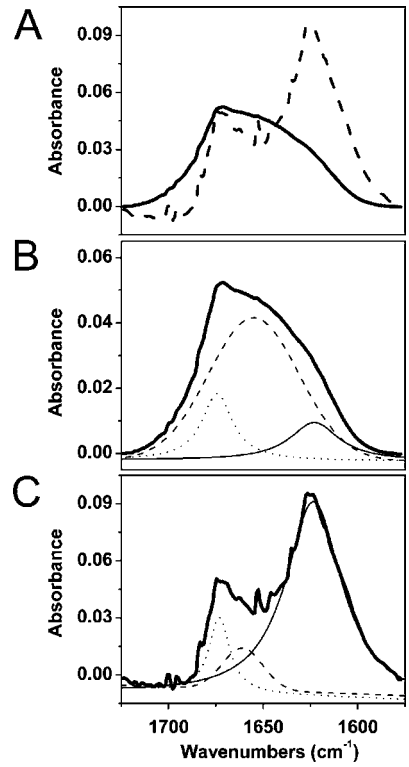

Figure 3. β-Sheet content of assemblies. (A) FTIR spectra of IAPP(11-25)WT (solid line) and IAPP(11-25)S20G (dashed line) in deuterated phosphate buffer at pH 7.5 and 25 °C. Both spectra were fit to three pseudo-Voigt bands, and the results are shown in (B) for IAPP(11-25)WT and in (C) for IAPP(11-25)S20G. In both figures, the bold lines show the data collected; the remaining lines represent the three contributing bands determined through fitting. In both cases, the band at 1674 cm^{-1} (dotted line) is indicative of residual trifluoroacetic acid and was used to normalize the spectra. (B) Two peptide amide I bands at 1622 (solid line) and 1654 cm^{-1} (dashed line) indicate the presence of parallel β-sheets and α-helical or disordered regions in the wild type peptide, respectively. (C) Two peptide amide I bands at 1623 (solid line) and 1661 cm^{-1} (dashed line) indicate the presence of parallel β-sheets and disordered regions, respectively, in the mutated peptide. The relative areas of the amide I bands clearly indicate that the S20G peptide forms more β-sheet than the wild type peptide.

(44) Wood, S. J.; Wetzel, R.; Martin, J. D.; Hurle, M. R. *Biochemistry* **1995**, *34*, 724–730.
(45) Moriarty, D. F.; Raleigh, D. P. *Biochemistry* **1999**, *38*, 1811–1818.
(46) Darnell, G.; Orgel, J. P.; Pahl, R.; Meredith, S. C. *J. Mol. Biol.* **2007**, *374*, 688–704.
(47) Kayed, R.; Bernhagen, J.; Greenfield, N.; Sweimeh, K.; Brunner, H.; Voelter, W.; Kapurniotu, A. *J. Mol. Biol.* **1999**, *287*, 781–796.
(48) Soldi, G.; Bemporad, F.; Torrassa, S.; Relini, A.; Ramazzotti, M.; Taddei, N.; Chiti, F. *Biophys. J.* **2005**, *89*, 4234–4244.
(49) Petty, S. A.; Volk, M. *Phys. Chem. Chem. Phys.* **2004**, *6*, 1022–1030.
(50) Grahnen, J. A.; Amunson, K. E.; Kubelka, J. *J. Phys. Chem. B* **2010**, *114*, 13011–13020.
(51) Zhang, M.; Fabian, H.; Mantsch, H. H.; Vogel, H. J. *Biochemistry* **1994**, *33*, 10883–10888.
(52) Fang, C.; Senes, A.; Cristian, L.; DeGrado, W. F.; Hochstrasser, R. M. *Proc. Natl. Acad. Sci. U.S.A.* **2006**, *103*, 16740–16745.
(53) Wimley, W. C.; Hristova, K.; Ladokhin, A. S.; Silvestro, L.; Axelsen, P. H.; White, S. H. *J. Mol. Biol.* **1998**, *277*, 1091–1110.
(54) Londergan, C. H.; Wang, J.; Axelsen, P. H.; Hochstrasser, R. M. *Biophys. J.* **2006**, *90*, 4672–4685.
(55) Radovan, D.; Smirnovas, V.; Winter, R. *Biochemistry* **2008**, *47*, 6352–6360.
(56) Khurana, R.; Fink, A. L. *Biophys. J.* **2000**, *78*, 994–1000.
(57) Lazo, N. D.; Downing, D. T. *Biochem. Biophys. Res. Commun.* **1997**, *235*, 675–679.
(58) Byler, D. M.; Susi, H. *Biopolymers* **1986**, *25*, 469–487.

25)S20G representing 91% of the total area assigned to peptide backbone vibrations. The dominant band at 1654 cm^{-1} in the spectrum of IAPP(11-25)WT is likely indicative of α-helix, which has been previously observed between 1650 and 1658 cm^{-1} in large proteins and poorly solvated peptides as would be present in aggregated assemblies.[58−60] This band overlaps with the disordered region, making it difficult to deconvolute the bands and discern exact percentages in the α-helix and random coil conformations. However, by taking together our CD and FTIR results, we conclude that IAPP(11-25)WT predominantly forms α-helical assemblies. The remaining band in the IAPP(11-25)S20G spectrum at 1661 cm^{-1} represents just 9% of the total area assigned to peptide backbone vibrations. We assign this to a disordered, non-hydrogen bonded conformation in the peptide. Frequencies above 1660 cm^{-1} have been assigned to unfolded structures of apomyoglobin,[59,61] to internal random coil segments in an α-helical coiled coil GCN4-P1′ under denaturing conditions,[62] and to irregular structures in chemically denatured RNaseA.[63]

The alignment of strands in the β-sheets deserves some comment. Antiparallel β-sheets are most commonly characterized by a pair of amide I bands at 1615−1620 cm^{-1} and at 1680−1690 cm^{-1} with the area of the latter being about 10% of the area of the lower frequency band.[64] Such a large splitting of the amide I band is caused by cross-strand transition dipole coupling and is unique to antiparallel β-sheets.[64] On the basis of the absence of the 1680−1690 cm^{-1} band, we conclude that the dominant structure in IAPP(11-25)S20G is parallel β-sheet.

Tinctorial Properties of Assemblies. We probed the ability of the IAPP(11-25)WT and IAPP(11-25)S20G assemblies to bind thioflavin T (ThT) and Congo red, two classic dyes for the detection of amyloid fibrils. ThT is a benzothiazole dye whose fluorescence increases dramatically upon binding to amyloid fibrils.[65,66] The basis for the enhancement is poorly understood but may lie in the elucidation of ThT−β-sheet interactions at the atomic level.[67,68] Examination of the IAPP(11-25)S20G solutions incubated over a period of 20 days shows dramatic enhancement of ThT fluorescence (Figure 4 and Figure S3 in the Supporting Information). In contrast, ThT fluorescence in the IAPP(11-25)WT and IAPP(11-25)S20P solutions is much weaker. Congo red is a diazo dye which undergoes a hyperchromatic shift in its absorbance spectrum upon binding to β-sheets in amyloid fibrils.[69] Figure S4 in the Supporting Information presents UV absorbance spectra of Congo red in the absence or presence of IAPP(11-25) peptides incubated for 20 days. Only in the presence of IAPP(11-25)S20G did Congo red become hyperchromatic.

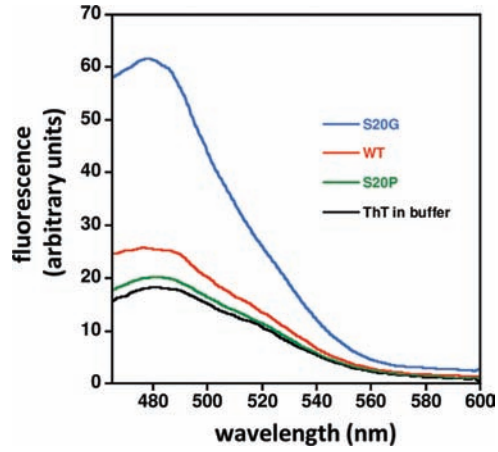

Figure 4. ThT fluorescence in the presence of assemblies. Fluorescence spectra of ThT in the absence and presence of IAPP(11-25) peptides that have been incubated at 4 °C for 20 days show that dramatic enhancement of fluorescence occurs only in the presence of assemblies formed by the IAPP(11-25)S20G. The final peptide concentration is approximately 7 μM.

Taking together our CD, FTIR, TEM, and dye binding results, we conclude that IAPP(11-25)S20P does not aggregate while IAPP(11-25)WT and IAPP(11-25)S20G self-assemble but in different ways. The WT peptide predominantly forms α-helical assemblies (Figures 2A and 3B). The S20G mutation induces the formation of more amyloid fibrils, consistent with previous studies using full-length IAPP.[70] Furthermore, we noted that the concentration of the α-helix-containing intermediate does not increase significantly in the S20G peptide (Figures 2B and 3C), suggesting that the S20G mutation facilitates the α-helix to β-sheet conformational rearrangement necessary for the formation of amyloid fibrils.

Monomeric States: Where Assembly Begins. To explain the differences in assembly competence among the three IAPP(11-25) peptides, we characterized the monomeric states of the IAPP(11-25) peptides by solution-state ^{1}H NMR. TOCSY and ROESY spectra of the three peptides obtained immediately after sample preparation show well-resolved cross peaks and good dispersion of chemical shifts (see Figure S5 in the Supporting Information). ^{1}H chemical shifts of the three peptides are shown in Table S2 in the Supporting Information.

To determine the secondary structure that may be present in the three peptides, we first analyzed interresidue ROE connectivities among the backbone NH, H^α, and H^β protons and three-bond *J*-coupling constants between NH and H^α protons ($^3J_{NH-H^\alpha}$). We did not observe $d_{\alpha N}(i,i+3)$, $d_{\alpha N}(i,i+4)$, $d_{\alpha\beta}(i,i+3)$, or long-range ROEs in the three peptides (Table S3 in the Supporting Information). The averages of the $^3J_{NH-H^\alpha}$ values are 7.1, 6.9, and 7.3 Hz for IAPP(11-25)WT, IAPP(11-25)S20G, and IAPP(11-25)S20P, respectively. For comparison, calculated $^3J_{NH-H^\alpha}$ values for residues in an α-helix and parallel β-sheet are 3.9 and 9.7 Hz, respectively.[71] Together, the ROE and *J*-coupling data suggest that the monomeric states of the IAPP(11-25) peptides do not contain stable, long-lived secondary structures.

To further explore the presence of local structure, we also calculated secondary chemical shifts ($\Delta\delta = \delta_{observed} - \delta_{random\ coil}$)[72] of the H^α protons (Figure 5). The H^α shifts depend

(59) Dyer, R. B.; Gai, F.; Woodruff, W. H.; Gilmanshin, R.; Callender, R. H. *Acc. Chem. Res.* **1998**, *31*, 709–716.
(60) Prestrelski, S. J.; Byler, D. M.; Liebman, M. N. *Biochemistry* **1991**, *30*, 133–143.
(61) Gilmanshin, R.; Williams, S.; Callender, R. H.; Woodruff, W. H.; Dyer, R. B. *Biochemistry* **1997**, *36*, 15006–15012.
(62) Manas, E. S.; Getahun, Z.; Wright, W. W.; DeGrado, W. F.; Vanderkooi, J. M. *J. Am. Chem. Soc.* **2000**, *122*, 9883–9890.
(63) Reinstadler, D.; Fabian, H.; Backmann, J.; Naumann, D. *Biochemistry* **1996**, *35*, 15822–15830.
(64) Krimm, S.; Bandekar, J. *Adv. Protein Chem.* **1986**, *38*, 181–364.
(65) Naiki, H.; Higuchi, K.; Hosokawa, M.; Takeda, T. *Anal. Biochem.* **1989**, *177*, 244–249.
(66) LeVine, H., III. *Protein Sci.* **1993**, *2*, 404–410.
(67) Biancalana, M.; Koide, S. *Biochim. Biophys. Acta* **2010**, *1804*, 1405–1412.
(68) Groenning, M. *J. Chem. Biol.* **2010**, *3*, 1–18.
(69) Klunk, W. E.; Jacob, R. F.; Mason, R. P. *Methods Enzymol.* **1999**, *309*, 285–305.
(70) Sakagashira, S.; Hiddinga, H. J.; Tateishi, K.; Sanke, T.; Hanabusa, T.; Nanjo, K.; Eberhardt, N. L. *Am. J. Pathol.* **2000**, *157*, 2101–2109.
(71) Wüthrich, K. *NMR of Proteins and Nucleic Acids*; John Wiley & Sons: New York, 1986.

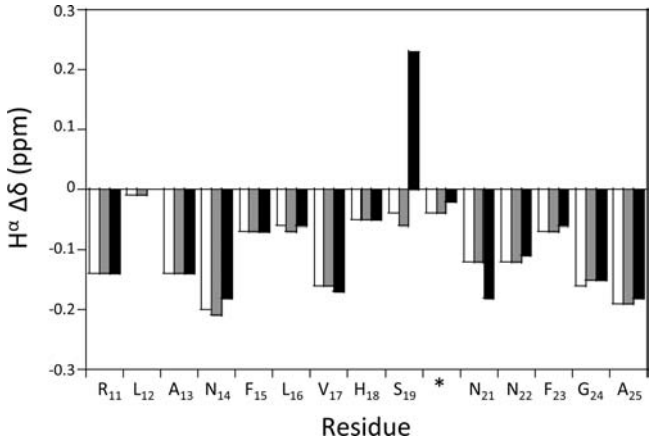

Figure 5. Detection of monomeric transient α-helices by NMR. H^{α} secondary chemical shifts ($\Delta\delta = \delta_{observed} - \delta_{random\ coil}$) for IAPP(11-25)WT (unshaded bars), IAPP(11-25)S20G (gray bars), and IAPP(11-25)S20P (black bars) calculated using $\delta_{random\ coil}$ values from acetyl-GGXGG-NH_2 peptides in 8 M urea.[87] The $\Delta\delta$ values are consistent with the presence of transient helices in IAPP(11-25)WT and IAPP(11-25)S20G and a transient helix−X−helix motif (X = Ser19 in the β conformation) in IAPP(11-25)S20P.

strongly on φ,ψ torsion angles such that $\delta_{observed}$ for a residue in an α-helix is upfield of $\delta_{random\ coil}$ while that for a residue in a β-sheet is downfield of $\delta_{random\ coil}$.[73] In IAPP(11-25)WT, all $\Delta\delta$ values are negative but not as negative as the $\Delta\delta$ value (~ -0.4 ppm) for a residue in a long-lived α-helix.[74] Together with the absence of $d_{\alpha N}(i,i+3)$, $d_{\alpha N}(i,i+4)$, and $d_{\alpha\beta}(i,i+3)$ ROEs, we conclude that IAPP(11-25)WT contains a transient α-helix, in agreement with previous NMR studies by the Miranker group showing a transient helix between residues 5 and 22 of rat IAPP[18] and across residues 5−19 of human IAPP.[20]

Glycine does not possess a side chain, and thus, the range of allowed (φ,ψ) torsion angles is much broader than for other residues.[75] However, we did not observe significant differences in H^{α} secondary chemical shifts (Figure 5) and ROE interactions (Table S3 in the Supporting Information) between IAPP(11-25)WT and IAPP(11-25)S20G peptides, suggesting that the conformational ensembles present in the two peptides are similar. Previous extensive replica exchange molecular dynamics simulations on the effects of the S20G mutation on IAPP(15-27) detected mainly random coil and small population of helices and β-hairpins with the β-turn centered at Gly20 and Asn21.[76] Our NMR data for IAPP(11-25)S20G do not include evidence for a β-hairpin. NMR studies of full-length human IAPP[20] and free-acid full-length IAPP in aqueous buffers at pH ∼6 also indicate the absence of β structure.[19]

Proline is unique among the naturally occurring amino acids in that its backbone contains a five-membered pyrrolidine ring,

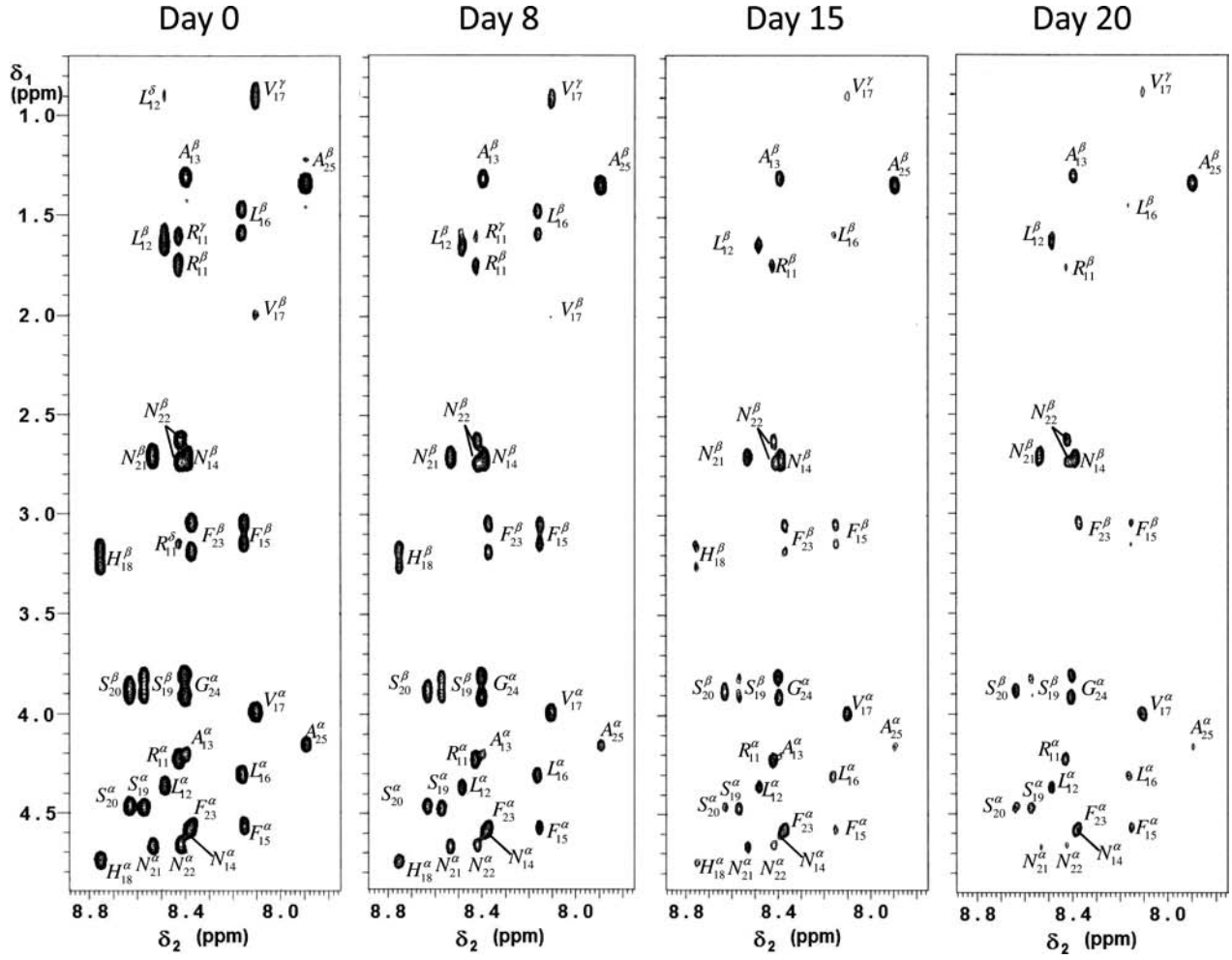

Figure 6. Time dependence of NMR spectra of IAPP(11-25)WT. TOCSY spectra of the WT peptide as a function of incubation time at 4 °C in 10 mM sodium phosphate buffer (pH 4.3) in 90% H_2O/10% D_2O show a decrease in cross-peak volumes consistent with the loss of transient α-helices to NMR-invisible assemblies. The peptide concentration is 133 μM.

allowing it to adopt either cis or trans peptide bond conformations.[77] On the NMR chemical shift time scale, Xaa−prolyl cis/trans bond isomerization is slow, and thus, two resonance frequencies can be observed for nuclear spins close to the bond.[78] In the fingerprint region of the TOCSY spectrum of IAPP(11-25)S20P, we observed two signals for His18 and Ser19 (Figure S5 in the Supporting Information). Integration of these signals indicates that only 10−15% of the cis isomer of Ser19−Pro20 imide bond is present. Thus, in the calculation of the H^{α} secondary chemical shifts of IAPP(11-25)S20P (Figure 5), we used chemical shifts for the trans isomer only. We noted that all residues preceding and following Ser19 have $\Delta\delta$ values consistent with the presence of α-helices, but Ser19 has a $\Delta\delta$ value indicative of a β conformation. Together with the absence of $d_{\alpha N}(i,i+3)$, $d_{\alpha N}(i,i+4)$, and $d_{\alpha\beta}(i,i+3)$ ROEs, we conclude that IAPP(11-25)S20P transiently samples a helix−X−helix (HXH) motif where two α-helices are linked by a single residue (Ser19) that is in a β conformation.

When found in α-helices, proline will kink[79] or break[80] the helix. Because of steric clashes with the pyrrolidine ring, the dihedral angles of the residue immediately preceding proline (the pre-Pro residue) are constrained within a narrow range that includes a small part of the α region and two small subsets of the β region.[75] Analysis of 837 HXH motifs obtained from nonhomologous sets of protein structures compiled from the Protein Data Bank (PDB) showed that a linker residue in the β conformation leads to a dramatic change in the relative orientation of the two helices, with bend angles >90° when proline is the residue in the X + 1 position.[80] As an example, the bend angle in the HXH motif found in residues 183−206 of gluthathione *S*-transferase (PDB ID 1OE8) (X = Ser196 and X + 1 = Pro197) is 107°.[80] For comparison, the bend angle in a standard Pro-kink is 21°.[81] The increase in bend angle in a HXH motif where X = Ser and X + 1 = Pro has been ascribed to the additional hydrogen bond between the hydroxyl group in the Ser side chain with the backbone carbonyl of the X − 4 residue.[80,82] As discussed below, the inability of IAPP(11-25)S20P to aggregate can be explained by this Ser-Pro induced helix break.

We then collected 1D and 2D (TOCSY and ROESY) spectra of IAPP(11-25)WT and IAPP(11-25)S20G peptides over time to characterize at the atomic level early events in aggregation. For control, spectra of IAPP(11-25)S20P were also acquired. TOCSY spectra of IAPP(11-25)WT, IAPP(11-25)S20G, and IAPP(11-25)S20P acquired over a span of 20 days are shown in Figure 6, Figure S6 in the Supporting Information, and Figure 7, respectively. In all spectra, no new cross peaks were detected. Line or peak broadening that would indicate exchange between monomers and larger assemblies was not observed. The spectra of IAPP(11-25)S20P did not change with time (Figure 7). In contrast, the cross-peak volumes in the spectra of IAPP(11-25)WT (Figure 6) and IAPP(11-25)S20G (Figure S6 in the Supporting Information) decreased with time. This decrease must result from the conversion of peptide monomers to assemblies whose peaks are broadened beyond detection due to their large size and hence long rotational correlation times. Our CD data suggest that these assemblies for the WT and S20G

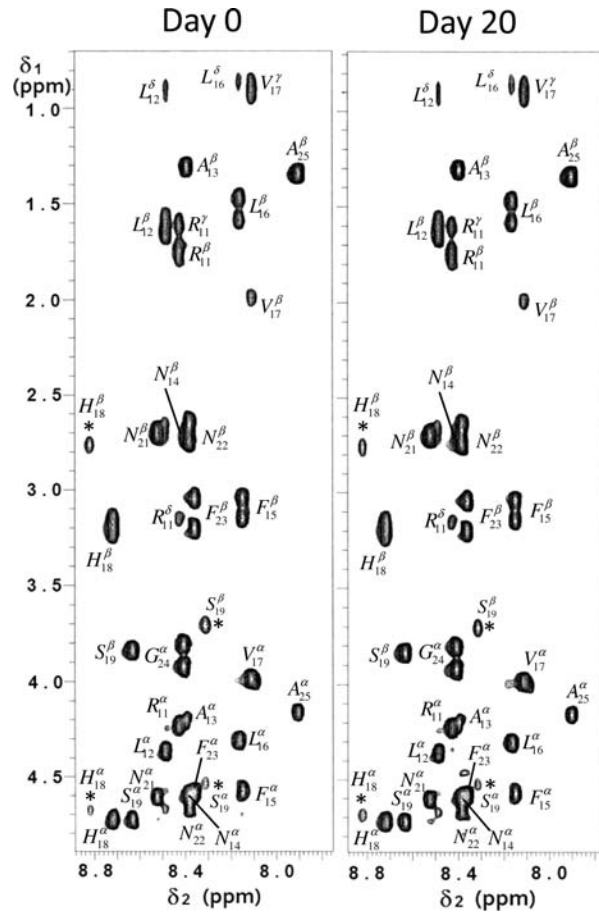

Figure 7. Abolishment of self-assembly by a proline substitution. Cross peaks in the TOCSY spectra of IAPP(11-25)S20P remained unchanged consistent with the absence of aggregation. The peptide concentration is 287 μM. Cross peaks with an asterisk (*) are due to the cis isomer of the Ser19−Pro20 imide bond.

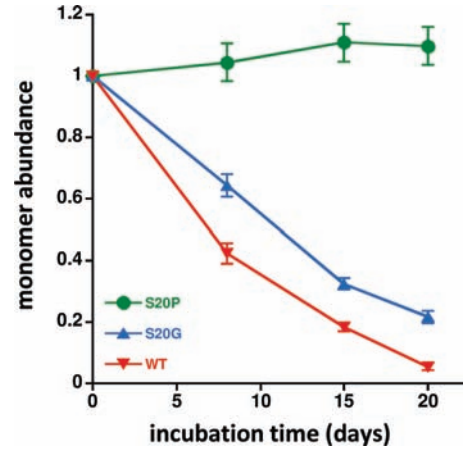

Figure 8. Effects of single amino acid substitutions on the loss of monomeric transient α-helices to self-assembly. The NH → H^{α} TOCSY cross-peak volumes were averaged over all residues in each peptide and reported relative to its initial value at day 0. The monomer abundance in IAPP(11-25)WT decreased more rapidly than in IAPP(11-25)S20G.

(72) Wishart, D. S.; Sykes, B. D.; Richards, F. M. *J. Mol. Biol.* **1991**, *222*, 311–333.
(73) Shen, Y.; Bax, A. *J. Biomol. NMR* **2007**, *38*, 289–302.
(74) Wishart, D. S.; Sykes, B. D. *Methods Enzymol.* **1994**, *239*, 363–392.
(75) Ho, B. K.; Brasseur, R. *BMC Struct. Biol.* **2005**, *5*, 14.
(76) Xu, W.; Jiang, P.; Mu, Y. *J. Phys. Chem. B* **2009**, *113*, 7308–7314.
(77) Grathwohl, C.; Wuthrich, K. *Biopolymers* **1976**, *15*, 2043–2057.
(78) Andreotti, A. H. *Biochemistry* **2003**, *42*, 9515–9524.
(79) Barlow, D. J.; Thornton, J. M. *J. Mol. Biol.* **1988**, *201*, 601–619.
(80) Deville, J.; Rey, J.; Chabbert, M. *Proteins* **2008**, *72*, 115–135.
(81) Cordes, F. S.; Bright, J. N.; Sansom, M. S. *J. Mol. Biol.* **2002**, *323*, 951–960.
(82) Deupi, X.; Olivella, M.; Govaerts, C.; Ballesteros, J. A.; Campillo, M.; Pardo, L. *Biophys. J.* **2004**, *86*, 105–115.

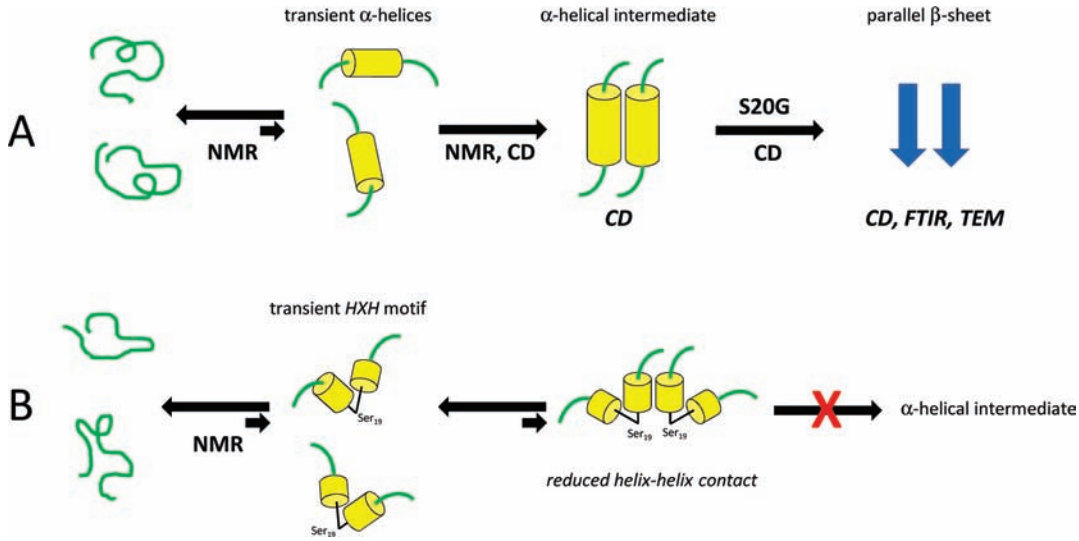

Figure 9. Schematic representation of resulting mechanism for peptide self-assembly and its abolishment by proline. (A) Transient α-helices self-assemble to form helical intermediates presumably stabilized by peptide−peptide interactions. The loss of transient helices is observable by NMR, and the presence of helical assemblies is detectable by CD. The ensuing conformational rearrangement to β-sheet, invisible by NMR but detectable by CD, is more facile in the peptide containing the S20G mutation primarily because of increased conformational flexibility resulting from the ability of glycine to access a wider range of φ,ψ torsion angles. (B) The S20P substitution leads to a transiently populated helix−X−helix motif, where X is Ser19 in the β conformation. The helix is broken into two with a bend angle >90°,[80] thereby reducing interhelical contact. The helical oligomers are unstable, and thus the ensuing steps to fibril formation are abolished. For clarity, only a dimer is shown in (A) and (B).

peptides are α-helix- and β-sheet-rich assemblies, respectively. Figure 8 presents the monomer abundance plotted against incubation time for the three IAPP(11-25) peptides. The abundance in IAPP(11-25)S20P remained essentially unchanged, consistent with the absence of self-assembly (see also Figure S7 in the Supporting Information). Interestingly, the monomer abundance for IAPP(11-25)WT decreased faster than those for IAPP(11-25)S20G.

Resulting Pathway for Peptide Self-Assembly and the Effect of Proline. The present results are summarized as follows: (1) Under conditions that favor polypeptide self-assembly, the 11−25 region of IAPP is exposed and flexible, suggesting that the initial intermolecular contacts are formed here. (2) Peptides containing this region, IAPP(11-25)WT and IAPP(11-25)S20G, self-assemble but in different ways: the WT peptide mainly forms α-helical assemblies while the S20G peptide predominantly forms fibrils. (3) Solution-state ^{1}H NMR indicates the presence of transient α-helices in IAPP(11-25)WT and IAPP(11-25)S20G. During the aggregation of these peptides, peaks due to intermediates including small oligomers were not observed. (4) IAPP(11-25)S20P, which does not aggregate, contains a transient HXH motif where X = Ser19 is in a β conformation. Figure 9A presents a schematic diagram of a pathway for the self-assembly of IAPP(11-25)WT and IAPP(11-25)S20G consistent with the present results. The pathway consists of two steps: the conversion of transient helices to helical assemblies which is detectable in the WT peptide by NMR, followed by the conversion of the helical assemblies to β-sheets which is highly favored in the S20G peptide and is invisible by NMR but detectable by CD. This pathway is similar to models proposed by others for IAPP in hydro and in the presence of model membranes.[6,83] In the first step, transient helices come together to form parallel α-helical assemblies presumably stabilized by intermolecular peptide−peptide interactions. Our NMR data show a more rapid decrease in monomer abundance with time in IAPP(11-25)WT than in IAPP(11-25)S20G (Figure 8), suggesting that the WT helical assemblies are more stable. Also, the conversion of the helical assemblies to β-sheet is slow in IAPP(11-25)WT and hence its concentration remains high throughout the time course of the fibrillation used here (Figure 2A). This conversion is more favored in IAPP(11-25)S20G presumably due to a greater conformational flexibility resulting from the ability of glycine to access a broader range of φ,ψ torsion angles. The serine-to-proline substitution at position 20 leads to a break in the helix. Because of reduced interhelical contacts (Figure 9B), the α-helical assemblies are unstable and, thus, fibril formation is abolished. To the best of our knowledge, this work is the first to provide mechanistic details for the inhibition of α-helical intermediates by proline.

The present work has implications for both the pathway of aggregation of IAPP and the development of therapeutic strategies that target IAPP. In addition to peptide−peptide interactions, transient α-helices can also be stabilized by peptide−membrane interactions.[84,85] A helical intermediate has been detected during the fibrillation of full-length IAPP in the presence of membranes,[6,86] with the helical region spanning residues 9−22, as determined by electron paramagnetic resonance.[86] Therapeutic strategies that target the helical intermediate require detailed knowledge of the folding and assembly of the intermediate. The results here indicate the availability of IAPP(11-25)WT for possible structure determination. Furthermore, the present study suggests that disrupting intermolecular helix−helix interactions as in IAPP(11-25)S20P may prevent the formation of oligomeric helical assemblies. This strategy

(83) Abedini, A.; Raleigh, D. P. *Phys. Biol.* **2009**, *6*, 015005.
(84) Nanga, R. P.; Brender, J. R.; Xu, J.; Veglia, G.; Ramamoorthy, A. *Biochemistry* **2008**, *47*, 12689–12697.
(85) Brender, J. R.; Hartman, K.; Reid, K. R.; Kennedy, R. T.; Ramamoorthy, A. *Biochemistry* **2008**, *47*, 12680–12688.
(86) Apostolidou, M.; Jayasinghe, S. A.; Langen, R. *J. Biol. Chem.* **2008**, *283*, 17205–17210.
(87) Schwarzinger, S.; Kroon, G. J.; Foss, T. R.; Wright, P. E.; Dyson, H. J. *J. Biomol. NMR* **2000**, *18*, 43–48.

may be applicable to other amyloidogenic proteins that contain transient α-helices including Aβ in AD and α-syn in PD.

Acknowledgment. This work was supported by the American Diabetes Association.

Supporting Information Available: Figures showing dot blot assay of IAPP(11-25) solutions, CD of IAPP(11-25)WT at a lower peptide concentration, ThT fluorescence at various time points, UV absorbance spectra of Congo red, representative TOCSY and ROESY spectra of the IAPP(11-25) peptides, TOCSY spectra of IAPP(11-25)S20G acquired as a function of incubation time at 4 °C, and SDS PAGE of IAPP(11-25)S20P solutions; tables presenting results of the LP/MS of IAPP at 25 °C and pH 5.5, ^{1}H chemical shifts of the IAPP(11-25) peptides, and summary of ^{1}H−^{1}H rotating-frame Overhauser enhancement interactions detected in ROESY spectra. This material is available free of charge via the Internet at http://pubs.acs.org.

JA1069882